1521-0111/102/2/92–105$35.00
MOLECULAR PHARMACOLOGY

dx.doi.org/10.1124/molpharm.122.000529
Mol Pharmacol 102:92–105, August 2022

MOLECULAR PHARMACOLOGY

Effects of Inhibitors of SLC9A-Type Sodium-Proton Exchangers on *Survival Motor Neuron 2* (*SMN2*) mRNA Splicing and Expression[S]

Sambee Kanda, Emily Moulton, and Matthew E.R. Butchbach

Division of Neurology, Nemours Children's Hospital Delaware, Wilmington, Delaware (S.K., E.M., M.E.R.B.); Department of Biological Sciences, University of Delaware, Newark, Delaware (S.K., M.E.R.B.); Center for Pediatric Research, Nemours Biomedical Research, Nemours Children's Hospital Delaware, Wilmington, Delaware (M.E.R.B.); and Department of Pediatrics, Thomas Jefferson University, Philadelphia, Pennsylvania (M.E.R.B.)

Received March 15, 2022; accepted May 9, 2022

ABSTRACT

Spinal muscular atrophy (SMA) is an autosomal recessive, pediatric-onset disorder caused by the loss of spinal motor neurons, thereby leading to muscle atrophy. SMA is caused by the loss of or mutations in the *survival motor neuron 1* (*SMN1*) gene. *SMN1* is duplicated in humans to give rise to the paralogous *survival motor neuron 2* (*SMN2*) gene. This paralog is nearly identical except for a cytosine to thymine transition within an exonic splicing enhancer element within exon 7. As a result, the majority of *SMN2* transcripts lack exon 7 (SMNΔ7), which produces a truncated and unstable SMN protein. Since *SMN2* copy number is inversely related to disease severity, it is a well established target for SMA therapeutics development. 5-(N-ethyl-N-isopropyl)amiloride (EIPA), an inhibitor of sodium/proton exchangers (NHEs), has previously been shown to increase exon 7 inclusion and SMN protein levels in SMA cells. In this study, NHE inhibitors were evaluated for their ability to modulate *SMN2* expression. EIPA as well as 5-(N,N-hexamethylene)amiloride (HMA) increase exon 7 inclusion in *SMN2* splicing reporter lines as well as in SMA fibroblasts. The EIPA-induced exon 7 inclusion occurs via a unique mechanism that does not involve previously identified splicing factors. Transcriptome analysis identified novel targets, including *TIA1* and *FABP3*, for further characterization. EIPA and HMA are more selective at inhibiting the NHE5 isoform, which is expressed in fibroblasts as well as in neuronal cells. These results show that NHE5 inhibition increases *SMN2* expression and may be a novel target for therapeutics development.

SIGNIFICANCE STATEMENT

This study demonstrates a molecular mechanism by which inhibitors of the sodium-protein exchanger increase the alternative splicing of *SMN2* in spinal muscular atrophy cells. NHE5 selective inhibitors increase the inclusion of full-length *SMN2* mRNAs by targeting *TIA1* and *FABP3* expression, which is distinct from other small molecule regulators of *SMN2* alternative splicing. This study provides a novel means to increase full-length *SMN2* expression and a novel target for therapeutics development.

Introduction

Proximal spinal muscular atrophy (SMA) is an early-onset neurodegenerative disease characterized by the loss of α-motor neurons in the anterior horn of the spinal cord, which leads to muscle weakness and atrophy (Crawford and Pardo, 1996; Tisdale and Pellizzoni, 2015). SMA is an autosomal recessive disease with an incidence of 1 in 6000–10,000 births (Pearn, 1978; Cuscó et al., 2002). SMA results from the loss or mutation of *survival motor neuron 1* (*SMN1*) con chromosome 5q13 (Lefebvre et al., 1995). Uniquely in humans, a large tandem chromosomal duplication has led to a second copy of this gene known as *survival motor neuron 2* (*SMN2*) (Lorson et al., 1999; Monani et al., 1999). *SMN2* is functionally distinguishable from *SMN1* by a single nucleotide difference (*SMN2 c.850C>T*) in exon 7 that disrupts an

This work was supported by National Institutes of Health Institute of General Medical Sciences [Grant P20-GM103446] (M.E.R.B.) and [Grant P20-GM103464] (M.E.R.B.), Nemours Foundation, and University of Delaware Graduate Research Fellowship.

No author has an actual or perceived conflict of interest with the contents of this article.

dx.doi.org/10.1124/molpharm.122.000529.

[S] This article has supplemental material available at molpharm.aspetjournals.org.

ABBREVIATIONS: ATXN1, ataxin-1; BLA, β-lactamase; COL3A, collagen IIIA; C_t, cycle threshold; DHCR7, 7-dehydrocholesterol reductase; DMA, 5-(N,N-dimethyl)amiloride; E, efficiency; EIPA, 5-(N-ethyl-N-isopropyl)amiloride; FABP3, fatty acid binding protein 3; FDA, Food and Drug Administration; FL-SMN, full-length SMN; FL-STRN3, full-length striatin-3; FOXM1, forkhead box protein M1; HMA, 5-(N,N-hexamethylene)amiloride; hnRNPA1, heterogeneous nuclear ribonucleoprotein A1; hTra2β1, transformer 2 β homolog; NHE, sodium/proton exchanger; PCR, polymerase chain reaction; PRKAR2B, protein kinase cAMP-dependent type II regulatory subunit β; RT-PCR, reverse-transcription polymerase chain reaction; SaM68, Src-associated in mitosis 68 kDa; SF2/ASF, splicing factor 2 homolog/alternative-splicing factor; SI, splicing factor; SMA, spinal muscular atrophy; SMN1, survival motor neuron 1; SMN2, survival motor neuron 2; SRp20, serine/arginine-rich splicing factor 20 kDa; STRN3, striatin 3; STRN3Δ89, STRN3 lacking exons 8 and 9; TIA1, T-cell–restricted intracellular antigen 1; TRPV4, transient receptor potential cation channel subfamily V member 4.

exonic splice enhancer. As a result, about 80%–90% of *SMN2* mRNAs lack exon 7 (*SMNΔ7*) and produce a protein that is both unstable and not fully functional (Lorson and Androphy, 2000; Burnett et al., 2009; Cho and Dreyfuss, 2010). Because 10%–20% of the *SMN2* gene product is fully functional (Lorson et al., 1999; Monani et al., 1999), increased genomic copies of *SMN2* inversely correlate with disease severity among individuals with SMA (Butchbach, 2016). Studies using transgenic mouse models for SMA have shown that increased *SMN2* copy number lessens the phenotypic severity of disease (Hsieh-Li et al., 2000; Monani et al., 2000; Michaud et al., 2010).

As *SMN2* is a major genetic modifier of SMA phenotype, it has become the primary target for the development of small molecule therapies for SMA (Cherry et al., 2014). *SMN2* gene expression can be regulated by increasing promoter activation, increasing inclusion of exon 7 in *SMN2* mRNA transcripts, and including translational readthrough of *SMNΔ7* mRNAs (Calder et al., 2016). Although there is currently no cure for SMA, a splice modifying oligonucleotide that increases *SMN2* exon 7 inclusion (nusinersen, Spinraza) recently received Food and Drug Administration (FDA) approval for SMA patients (Finkel et al., 2017; Mercuri et al., 2018). Splice-modifying oligonucleotides, however, have suboptimal properties, including not being able to cross the blood-brain barrier, not being orally bioavailable, potentially being toxic at high doses, and being expensive to manufacture (Sumner and Crawford, 2018). Despite these exciting advances, other therapies are needed, particularly if they are complementary to these current therapeutic options.

Small molecule inducers of *SMN2* exon 7 inclusion have been identified. NVS-SM1 (branaplam) is a small molecule *SMN2* exon 7 splicing modulator that is orally bioavailable and central nervous system penetrant (Palacino et al., 2015). The pyridopyrimidinone class of small molecule modulators of *SMN2* exon 7, including RG7800 and RG7916 (risdiplam), have also shown efficacy in cell culture as well as in animal models for SMA (Naryshkin et al., 2014; Feng et al., 2016; Ratni et al., 2016; Woll et al., 2016; Sivaramakrishnan et al., 2017; Ratni et al., 2018; Wang et al., 2018). Risdiplam (Evrysdi; Genetech and Roche) was recently approved by the FDA for treating SMA patients (Baranello et al., 2021). Other classes of small molecules have been identified as modulators of *SMN2* exon 7 splicing. 5-(N-ethyl-N-isopropyl)amiloride (EIPA), an inhibitor of sodium/proton exchangers (NHEs, also known as SLC9A family), upregulates *SMN2* expression in SMA lymphoblastoid cells by increasing the inclusion of exon 7 in *SMN2* transcripts (Yuo et al., 2008). In this study, we examine the effects of other NHE inhibitors—both structurally related to EIPA as well as other classes of inhibitors—on *SMN2* alternative splicing at exon 7 and *SMN* expression in SMA cells. The modulatory effects of EIPA and its analogs are also compared against RG7800, a well characterized *SMN2* exon 7 splicing modulator.

Materials and Methods

Test Compounds. Amiloride, cariporide, EIPA, 5-(N,N dimethyl)amiloride (DMA), and zoniporide were obtained from Cayman Chemicals (Ann Arbor, MI), and 5-(N, N-hexamethylene)amiloride (HMA) was purchased from Sigma-Aldrich (St. Louis, MO). The structures of the amiloride test compounds are shown in Fig. 1. RG7800 was obtained from MedKoo Biosciences, Inc (Morrisville, NC). All stock solutions were made by dissolving the compound in DMSO (Sigma-Aldrich).

Cell Culture. Fibroblast cells derived from type II SMA patients (GM03813, GM22592, and AIDHC-SP22) have a homozygous deletion of *SMN1* and three copies of *SMN2* (Stabley et al., 2015; Stabley et al., 2017). GM03814 fibroblasts (Scudiero et al., 1986) were derived from the carrier mother of GM03813, with one copy of *SMN1* and five copies of *SMN2* (Stabley et al., 2015). GM03813, GM22592, and GM03814 fibroblasts were obtained from Coriell Cell Repositories (Camden, NJ), and the other fibroblast lines were generated at Nemours Children's Hospital Delaware (Stabley et al., 2017). All fibroblast lines were authenticated using short tandem repeat profiling and digital polymerase chain reaction (PCR) (Stabley et al., 2017). The *SMN2* exon 7 splicing reporter cell line NSC-34:SMN2:Mg2:bla5.3 (Andreassi et al., 2001) was obtained from Vertex Pharmaceuticals (Boston, MA).

Fibroblast lines as well as NSC-34:SMN2:Mg2:bla5.3 cells were maintained in Dulbecco's modified essential medium (Life Technologies, Grand Island, NY) containing 10% EquaFETAL (Atlas Biologicals; Fort Collins, CO), 2 mM L-glutamine (Life Technologies), and 1% penicillin-streptomycin (Life Technologies). All cell lines were maintained in a humidified chamber at 37°C with 5% CO_2.

***SMN2* Exon 7 Splicing Reporter Assay.** NSC-34:SMN2:Mg2:bla5.3 cells (Andreassi et al., 2001) were seeded onto black-walled, clear-bottom 96-well tissue culture plates (Santa Cruz Biotechnology, Dallas, TX) at a density of 5×10^4 cells per cm^2. Drug compounds ($n = 4$ per dose) were added to serum-free medium at a dilution of 1:500. One-hundred microliters of drug-containing medium was then added to maintenance medium over the seeded NSC-34 cells. After incubation for 19 hours, media containing drug compounds was aspirated, and 100 μl of fresh maintenance medium was added to each well. Twenty microliters of 6X CCF2-AM loading solution (GeneBlazer In Vivo Detection Kit, Life Technologies; containing 6 μm CCF2-AM and 12 mM probenecid) were added to each of the assay wells, and plates were incubated at room temperature for 2 hours before the plates were read on a Victor ×4 (Perkin Elmer, Waltham, MA) fluorescence plate reader (λ_{ex} = 405 nm, λ_{em} = 530 nm, and λ_{em} = 460 nm). The 460-nm:530-nm fluorescence ratios were then calculated for each sample.

Drug Treatment of Cells. Fibroblasts were seeded 24 hours prior to drug treatment at a density of 3.2×10^4 cells per well in a 6-well plate for RNA analysis and of 4.0×10^5 cells per dish in a 10-cm dish for protein analysis. Test compounds were added to each sample at a 1:1000 dilution, and compound-containing medium was replaced every 24 hours during the 5-day treatment period. Cells were then harvested 24 hours after last drug compound treatment.

RNA Isolation. Total RNA was extracted from cell pellets using the RNeasy Mini kit (QIAGEN; Germantown, MD) per the manufacturer's instructions. RNA quality was assessed using a 2100 Bioanalyzer (Applied Biosystems).

***SMN* Exon 7 Inclusion Assay.** First-strand cDNA was synthesized from total RNA (500 ng) using the iScript cDNA Synthesis Kit (Bio-Rad, Hercules, CA) as described previously (Gentillon et al., 2017). PCRs were run for sample cDNAs using GoTaq Green Polymerase Mix (Promega; Madison, WI) with the following primer sets (Integrated DNA Technologies; Coralville, IA): *SMN*, SMNex6 (F) 5′-cccatatgtccagattctcttgat-3′; SMNex8(R) 5′-ctacaacacccttctcacag-3′; and *human collagen-IIIA* (*COL3A*), COL3A (F) 5′-gctctgcttcatcccactatt-3′; COL3A(R) 5′-ggaataccagggtcaccattt-3′. PCR products were resolved through a 2% agarose gels via electrophoresis. Images were captured with an AlphaImager gel documentation station (ProteinSimple, San Jose, CA), and band intensities were quantified using Image J 1.45s (National Institutes of Health, Bethesda, MD).

Quantitative Reverse Transcriptase-Polymerase Chain Reaction (qPCR). qPCR was completed for each treated sample using the iScript cDNA Synthesis Kit and the Bullseye EvaGreen qPCR MasterMix (Midsci, Valley Park, MO) as described previously

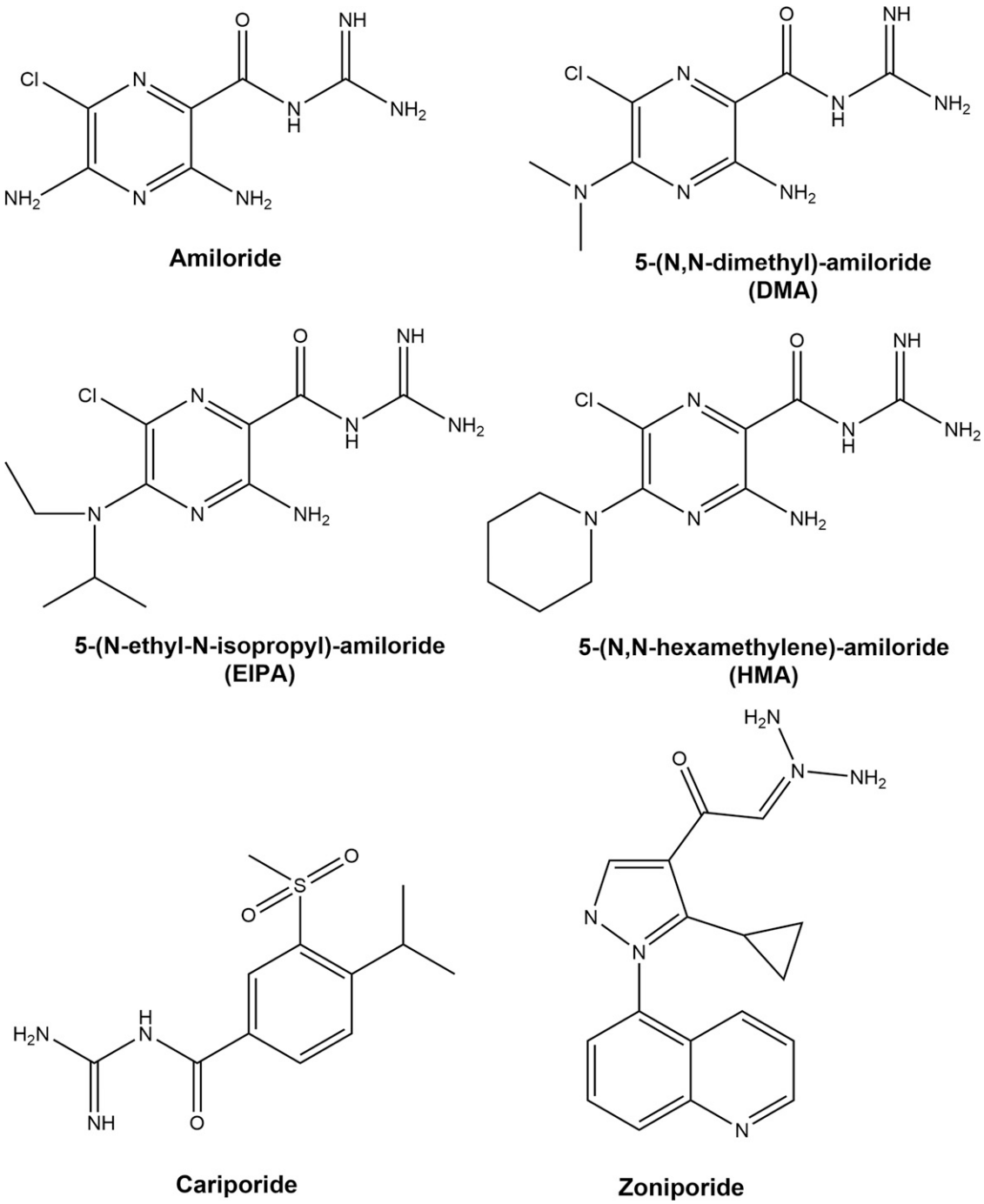

Fig. 1. Chemical structures of the SLC9A-type NHE inhibitors tested.

(Gentillon et al., 2017). Each sample was assayed in triplicate. The following primer sets were used: *full-length SMN* (*FL-SMN*) (SMNex6F) 5′-ccatatgtccagattctcttgatga-3′, (SMNex78R) 5′-atgccagcatttctccttaa ttta-3′; *SMN*Δ*7* (SMNex6F), (SMNex68R) 5′-atgccagcatttccatataa tagc-3′; *full-length striatin-3* (*FL-STRN3*) (STRN3F) 5′-ggaagaaaggg gtgaagagg-3′, (STRN3R) 5′-tgattcctgaagggatgtgg-3′; *STRN3 lacking exons 8 and 9* (*STRN3*Δ*89*) (STRN3D89F) 5′-cagaatgggctgaaccaataa-3′, (STRN3D89R) 5′-accgtcaagtctgcaaggtc-3′; *forkhead box protein M1A* (*FOXM1A*) (FOXM1AF) 5′-gaacatgaccatcaaaaccgaactc-3′, (FOXM1AR) 5′-aaattaaacaagctggtgatgggtg-3′; (*FOXM1B*) (FOXM1BF) 5′-ggaccagg tgtttaagcagcag-3′, (FOXM1BR) 5′-caatgcggactcgcttgctat-3′; (*FOXM1C*) (FOXM1CF) 5′-ttgcccgagcagttggaatca-3′, (FOXM1CR) 5′-tcctcagctag cagcaccttg-3′; *heterogeneous nuclear ribonucleoprotein A1* (*hnRNPA1*) (hnRNPA1-F) 5′-agggcgaaggtaggctggca-3′, (hnRNPA1-R) 5′-gcttcc tcagctcttcgggct-3′; *transformer 2 β homolog* (*hTra2β1*) (hTRA2bF) 5′-ca catcgaccggcgacagca-3′ (hTRA2bR) 5′-ccccgatccgtgagcacttcc-3′; *splicing factor-2 homolog/alternative-splicing factor* (*SF2/ASF*) (hSF2ASF-F) 5′-cagagtggttgtctctg-3′, (hSF2ASF-R) 5′-ctccacgacaccagtgcc-3′; *Src-associated in mitosis 68 kDa* (*SaM68*) (hSAM68F) 5′-atctctgtaattgg gaaagggc-3′, (hSAM68R) 5′-agagcataagcctcacatgg-3′; *serine/arginine-rich splicing factor 20 kDa* (*SRp20*) (hSRp20F) 5′-atgcatcgtgattcctg-3′, (hSRp20R) 5′-ctgcgacgaggtggagg-3′; *T-cell–restricted intracellular antigen-1* (*TIA1*) (TIA1-F) 5′-cagcgttcacaagatcatttcc-3′, (TIA1-R) 5′-tcccttagactttcctgttgc-3′; *fatty acid binding protein 3* (*FABP3*) (FABP3-F) 5′-aaatgggacgggcaagag-3′, (FABP3-R) 5′-tgcctctttctcataagtgcg-3′; *7-dehydrocholesterol reductase* (*DHCR7*) (DHCR7-F) 5′-gcaacccaa

cattcccaaag-3′, (DHCR7-R) 5′-agtgaaaaccagtccacctc-3′; *transient receptor potential cation channel subfamily V member 4* (*TRPV4*) (TRPV4-F) 5′-acctttccgattcctgctc-3′, (TRPV4-R) 5′-tcctcattgcacaccttcatg-3′; *ataxin-1* (*ATXN1*) (ATXN1-F) 5′-catccagagtgcagagataagc-3′, (ATXN1-R) 5′-ctctaccaaaacttcaacgctg-3′; and *protein kinase cAMP-dependent type II regulatory subunit β* (*PRKAR2B*) (PRKAR2B-F) 5′-tgatcaaggtgacgatggtg-3′, (PRKAR2B-R) 5′-tgtacattaaggccagttcgc-3′. Primers for the human reference transcripts *β-actin*, *large ribosomal protein P0*, and *glyceraldehyde-3-phosphate dehydrogenase* were purchased from Real Time Primers LLC (Elkins Park, PA).

The relative transcript levels were calculated using the efficiency-adjusted $2^{-\Delta\Delta Ct}$ method (Schmittgen and Livak, 2008; Yuan et al., 2008). The PCR efficiency (E) for each primer set was calculated from the slope of a cycle threshold (C_t) versus $\log_{10}$(cDNA serial dilution) curve ($E = 10^{[-1/slope]}$) (Pfaffl, 2001). $\Delta C_{t,adjusted}$ is the difference between the adjusted C_t ($C_{t,measured} \times E$) for the target transcript and the geometric mean of the adjusted C_t values for the three reference genes, and $\Delta\Delta C_t$ is defined as the difference between the ΔC_t for the SMA sample and the ΔC_t for the control sample.

Immunoblot. Protein extracts were generated from cell pellets as described previously (Gentillon et al., 2017). Protein extracts from treated cells (15 μg protein/lane) were resolved from miniPROTEAN TGX gradient precast acrylamide gels (BioRad) via electrophoresis as described previously (Gentillon et al., 2017). The resolved proteins were then transferred onto polyvinylidene difluoride membranes via electroblotting. Immunoblotting was completed as described in (Gentillon et al., 2017). The following antibodies were used in this study: mouse anti-SMN monoclonal antibody (1:2000; clone 8, BD Biosciences), mouse anti–β-actin monoclonal antibody (1:10,000; clone AC15, Sigma-Aldrich, St. Louis, MO), horseradish peroxidase-conjugated anti-mouse and anti-rabbit secondary antibodies (1:5000; Rockland Immunochemicals, Inc., Gilbertsville, PA). After extensive washing, the bound antibody was detected by chemiluminescence using either Western Sure ECL Substrate (LiCor, Lincoln, NE) or SuperSignal West Femto (Thermo Scientific) kits and captured with the C-DiGit Blot Scanner (LiCor). Band intensities, defined as the band signal divided by the band area, were measured using the Image StudioTM Lite software (LiCor). The measured band areas were the same for each sample on a blot. Band intensities for the target protein (SMN) were divided by those for the reference protein (β-actin) to obtain normalized band intensities. To measure the relative protein level for a sample, the normalized band intensity for the drug-treated sample was divided by the normalized band intensity for the control sample (DMSO-treated cells).

Microarray. cDNAs from treated RNA samples—with RNA integrity numbers greater than 9.0—were prepared using the GeneChip WT PLUS Reagent Kit (Applied Biosystems, Foster City, CA). Double-stranded cDNA was synthesized from 100 ng total RNA using a random primer that incorporated a T7 promoter. This double-stranded cDNA was then used as a template to generate cRNA via a 16-hour in vitro transcription reaction followed by purification with magnetic beads. Single-stranded cDNA was regenerated from this cRNA through a random primed reverse transcription using a deoxynucleoside triphosphate mix containing deoxyuridine triphosphate. After RNA hydrolysis with RNase H, the cDNA was purified using magnetic beads and then enzymatically fragmented with a mixture of uracil-DNA glycosylase and apyrinic/apyrimidinic endonuclease 1. This fragmented cDNA was then end labeled with a biotinylated dideoxynucleotide using terminal transferase. Fragmented, biotinylated cDNA was added to a hybridization cocktail, denatured, loaded on a Clariom D human GeneChips, and hybridized for 16 hours at 45°C and 60 rpm. Following hybridization, the chips were washed and stained using the preprogrammed FS450_0001 protocol. The stained chips were scanned at 532 nm with a GeneChip Scanner 3000 (Applied Biosystems).

The resultant data were analyzed with the TAC 4.0 software (Applied Biosystems). The raw data have been deposited into the National Center for Biotechnology Information Gene Expression Omnibus (Barrett et al., 2013) under the accession number GSE179861. Identification of biologic pathways and upstream regulators was completed using Ingenuity Pathway Analysis (version 21901358; QIAGEN Redwood City, Inc., Redwood City, CA) as described previously (Maeda et al., 2014). Biologic function and canonical pathways were determined to be over-represented using the Fisher exact test with a false discovery rate correction ($P \leq 0.05$). Upstream regulators were considered as being activated if their z-scores were greater than or equal to 2.0 or inhibited if they were less than or equal to −2.0 (Krämer et al., 2014).

Statistical Analysis. Data are expressed as mean plus or minus standard error. Parametric data were analyzed by ANOVA with a Holm-Sidak (expression analysis) post hoc test. Statistical significance was set at $P \leq 0.05$. Comparisons between data were performed with Sigma Plot v.12.0 or SPSS v.22.0.

Results

Effects of NHE Inhibitors on *SMN2* Exon 7 Alternative Splicing. To determine the effect of NHE inhibitors on increasing *SMN2* expression, we first examined their effects on the inclusion of *SMN2* exon 7. Using a *SMN2* exon 7 splicing reporter assay established in motor neuron–like NSC-34 cells (Andreassi et al., 2001), we measured the effects of amiloride, DMA, EIPA, HMA, cariporide, and zoniporide (Fig. 1) on β-lactamase (BLA) activity—a marker for *SMN2* exon 7 inclusion. The EIPA and HMA significantly increased exon 7 inclusion, as shown by an increase in the λ_{460nm} to λ_{530nm} fluorescence ratio, in these reporter cells (Fig. 2A). Amiloride, cariporide, and zoniporide, on the other hand, significantly reduced BLA activity.

We also examined the effect of NHE inhibitors on the inclusion of exon 7 in *SMN2* mRNAs in a SMA intracellular environment by using patient-derived fibroblasts. GM03813 type II SMA fibroblasts (Scudiero et al., 1986) were treated with different concentrations of amiloride, DMA, EIPA, HMA, zoniporide, or cariporide for 5 days. After treatment, *SMN2* exon 7 inclusion was measured via reverse-transcription polymerase chain reaction (RT-PCR) using primers spanning exons 6 through 8 of *SMN2*. *COL3A* transcript levels were used as a loading control as it is highly and constitutively expressed in fibroblast cells (Heier et al., 2007). As shown in Fig. 2B, the proportion of *FL-SMN* (top band) relative to *SMNΔ7* (bottom band) transcripts was increased in SMA fibroblasts treated with EIPA and HMA but not in any of the other NHE inhibitors. HMA was more potent at increasing *SMN2* exon 7 inclusion than EIPA (Fig. 2C).

There are 5 different isoforms of SLC9A-type Na^+/H^+ antiporters (*NHE1*, *NHE2*, *NHE3*, *NHE4*, and *NHE5*) that are present on the plasma membrane (Masereel et al., 2003). Using RT-PCR, we determined the SLC9A isoform expression profiles for NSC-34 cells as well as for GM03813 and GM03814 fibroblasts. NSC-34 cells as well as fibroblast cell lines express predominantly *NHE1* and *NHE5* (Supplemental Fig. 1).

Effects of NHE Inhibitors on *SMN2* Expression in Type II SMA Fibroblasts. We treated GM03813 type II SMA fibroblasts with different concentrations (0.1–10 μM) of the NHE inhibitors for 5 days. *FL-SMN* and *SMNΔ7* transcript levels were measured by qPCR. EIPA and HMA significantly increase *FL-SMN* mRNA levels in GM03813 cells to about 80% of the amount of *FL-SMN* seen in carrier fibroblasts (GM03814) (Fig. 3A). Amiloride, cariporide, and zoniporide, however, reduced the abundance of *FL-SMN* transcripts in

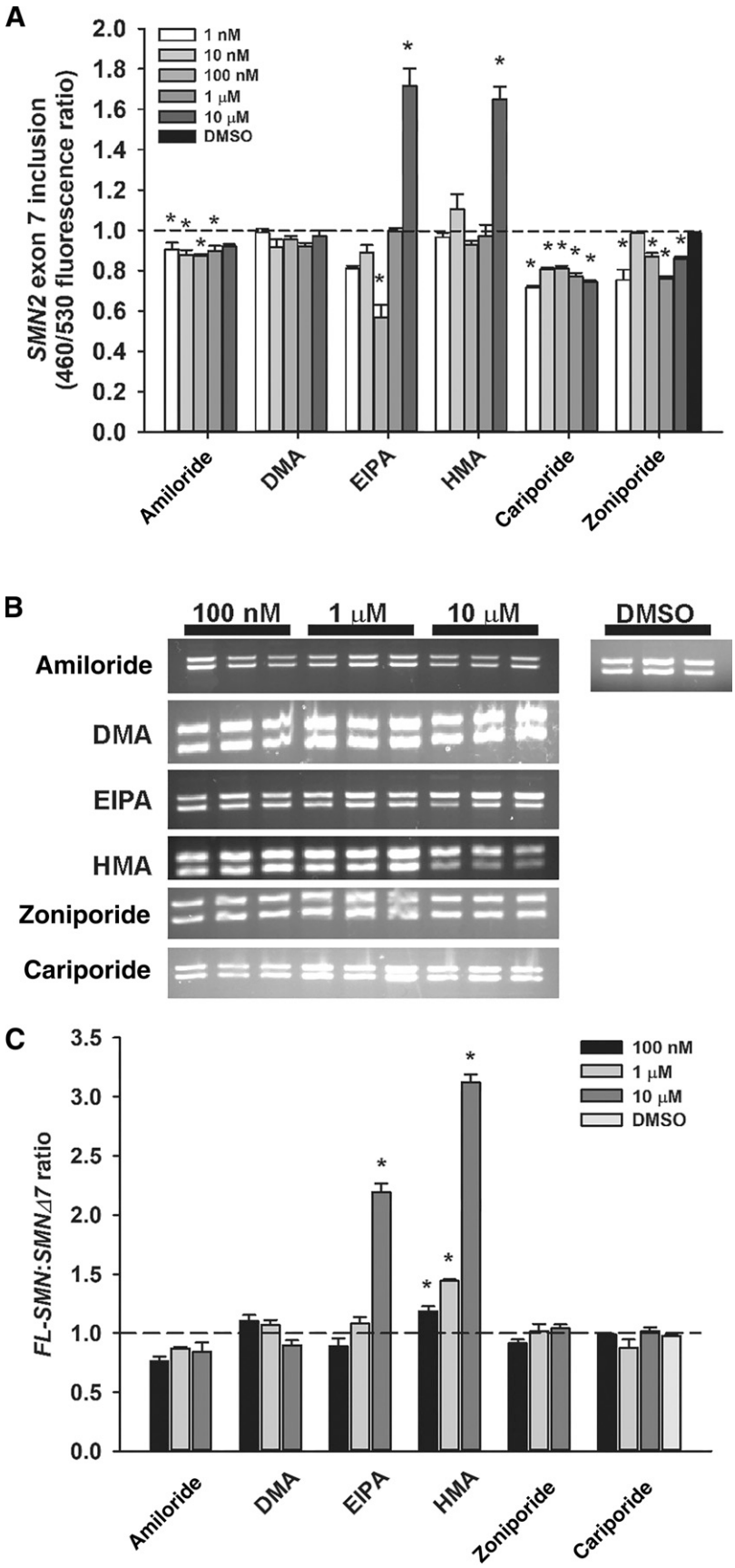

Fig. 2. Effects of NHE inhibitors on SMN2 alternative splicing. (A) *SMN2* exon 7 inclusion reporter cells (NSC-34:SMN2:Mg2:bla5.3) were treated with varying concentrations of the NHE inhibitors amiloride, DMA, EIPA, HMA, cariporide, or zoniporide (1 nM to 10 μM; $n = 4$ per dose) or DMSO for 19 hours. BLA activity was measured fluorimetrically. (B and C) Effect of NHE inhibitors on *SMN2* exon 7 inclusion in type II SMA fibroblasts. Type II SMA fibroblasts (GM03813) were treated with varying concentrations (100 nM to 10 μM; $n = 3$ per group) of NHE inhibitors or DMSO for 5 days ($n = 3$ per treatment group). After total RNA isolation, samples were analyzed for relative amounts of *FL-SMN* and *SMNΔ7* transcripts by RT-PCR and agarose gel electrophoresis. *COL3A* served as a loading control in this assay. The relative amounts of *FL-SMN* and *SMNΔ7* transcripts were also measured on carrier fibroblasts (GM03814). The asterisk (*) denotes a statistically significant ($P < 0.05$) difference between NHE inhibitor- and vehicle-treated cells.

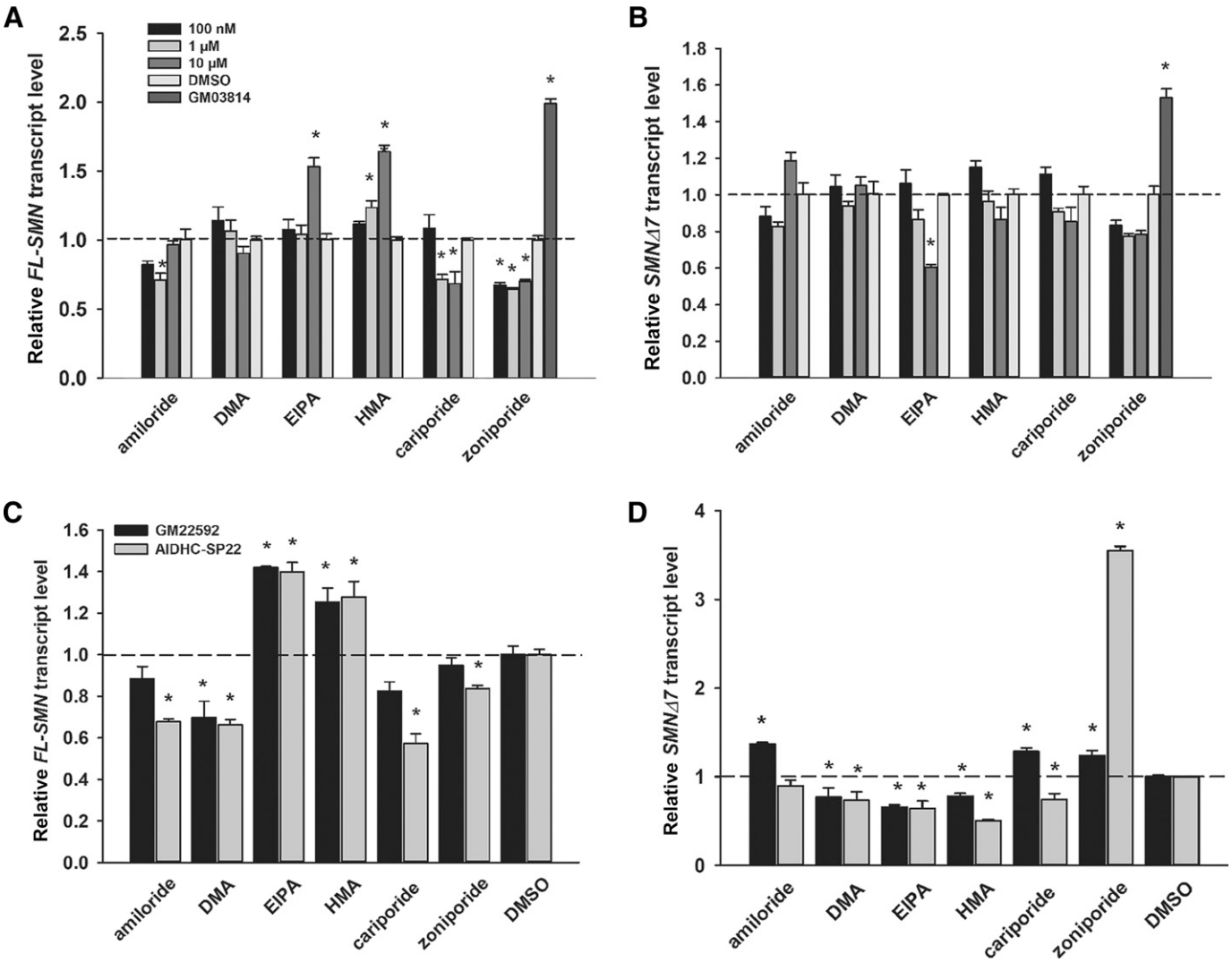

Fig. 3. Effects of NHE inhibitors on expression of FL-SMN and SMNΔ7 mRNA transcripts in SMA patient-derived fibroblasts. GM03813 type II SMA fibroblasts were treated with different concentrations of NHE inhibitors (100 nM to 10 μM; $n = 3$ per dose) or DMSO for 5 days. Changes in *FL-SMN* (A) or *SMNΔ7* (B) transcript levels were measured via quantitative RT-PCR with *β-actin*, *glyceraldehyde-3-phosphate dehydrogenase*, and *large ribosomal protein P0* serving as reference transcripts. *FL-SMN* and *SMNΔ7* transcript levels were also measured in GM03814 carrier fibroblasts. Changes in *FL-SMN* (C) or *SMNΔ7* (D) transcript levels were measured in two other type II SMA fibroblast lines (GM22592 and AIDHC-SP22) treated with NHE inhibitors (10 μM; $n = 3$ per inhibitor) for 5 days. All transcript levels were expressed relative to DMSO-treated GM03813 cells (dashed line). The asterisk (*) denotes a statistically significant ($P < 0.05$) difference between NHE inhibitor- and vehicle-treated cells.

SMA fibroblasts. EIPA was the only NHE inhibitor that significantly reduced the levels of *SMNΔ7* mRNA in treated cells (Fig. 3B). To demonstrate that these observations were not unique to a single SMA cell line, we measured the effects of the NHE inhibitors on *FL-SMN* and *SMNΔ7* transcript levels in two other type II SMA fibroblast lines— GM22592 and AIDHC-SP22. EIPA and HMA also increased *FL-SMN* transcripts in GM22592 and AIDHC-SP22 cells, indicating that their effects on *SMN2* mRNA regulation are cell-line independent (Fig. 3C). *SMNΔ7* transcript levels were also reduced in AIDHC-SP22 and GM22592 fibroblasts treated with EIPA or HMA (Fig. 3D).

We measured SMN protein levels of GM03813 type II SMA fibroblasts treated with the aforementioned NHE inhibitors for 5 days (Fig. 4). Amiloride, cariporide, and zoniporide had marginal effects on SMN protein levels in these cells. EIPA and HMA increased SMN protein levels in GM03813 fibroblasts, with EIPA showing a maximal effect at 10 μM, whereas the maximal effect of HMA was observed at 1 μM. Interestingly, DMA also increased SMA protein levels in SMA fibroblasts even though it had no effect on *FL-SMN* mRNA levels nor on exon 7 inclusion. This observation suggests that the DMA affects SMN gene regulation at a different level from EIPA and HMA.

Effects of NHE Inhibitors on Alternative Splicing of *STRN3* and *FOXM1* in SMA Fibroblasts. We measured the effects of the NHE inhibitors on the alternative splicing of other transcripts—aside from *SMN2*—that are affected by the pyridopyridinone RG7800 (Ratni et al., 2016; Woll et al., 2016) to determine if EIPA and HMA operate via a similar mechanism to promote exon 7 inclusion. *STRN3* has a similar pre-mRNA structure to the *SMN2* exon 7:intron 7 junction, and RG7800 increases the inclusion of *STRN3* exons 8 and 9 (Naryshkin et al., 2014; Sivaramakrishnan et al., 2017).

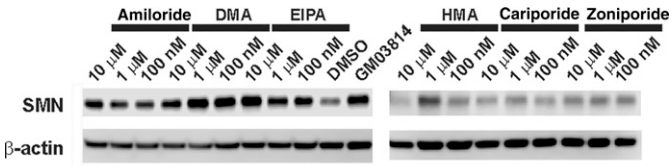

Fig. 4. Effects of NHE inhibitors on SMN protein levels in SMA fibroblasts. GM03813 type II SMA fibroblasts were treated with different concentrations of NHE inhibitors (100 nM to 10 μM; $n = 3$ per dose) or DMSO for 5 days. Changes in SMN protein levels were measured via immunoblot using β-actin as a reference protein. SMN protein levels were also measured in GM03814 carrier fibroblasts.

There are 3 isoforms of *FOXM1* generated by alternative splicing of exons Va and VIIa: *FOXM1A* (which contains both exons Va and VIIa), *FOXM1B* (which contains neither exon), and *FOXM1C* (which contains only exon Va) (Liao et al., 2018). RG7800 increased the abundance of *FOXM1A* while reducing *FOXM1C* levels (Ratni et al., 2018).

The levels of *STRN3* and *FOXM1* splice variants were measured in GM03813 type II SMA fibroblasts treated with amiloride, EIPA, HMA, or RG7800 for 5 days. EIPA and HMA had no effect on the amount of *FL-STRN3* mRNA, whereas amiloride significantly increased *FL-STRN3* transcript levels (Fig. 5A). RG7800 also increased the abundance of *FL-STRN3* transcripts in treated SMA fibroblasts. Interestingly, all NHE inhibitors tested increased *STRN3Δ89* mRNA levels (Fig. 5B), whereas RG7800 reduced the amount of *STRN3Δ89* transcripts. None of the NHE inhibitors increased the levels of *FOXM1A* in SMA fibroblasts (Fig. 5C). EIPA but not amiloride nor HMA significantly decreased *FOXM1C* transcript levels in SMA fibroblasts (Fig. 5D). *FOXM1B* transcripts could not be detected in fibroblast samples (data not shown). Predictably, RG7800 increased relative *FOXM1A* levels and reduced the amount of *FOXM1C* transcript levels in treated cells (Fig. 5, C and D). The mechanism of action of EIPA and HMA on the alternative splicing of *SMN2* exon 7, therefore, is distinct from that used by RG7800.

Effects of NHE Inhibitors on Expression of Regulators of *SMN2* Exon 7 Splicing. To understand the mechanism of action for the increased inclusion of exon 7 in *SMN2* transcripts induced by EIPA and HMA, we first examined the effects of NHE inhibitors on the expression of previously identified proteins that modulate the splicing of *SMN2* at exon 7. We focused on the following splicing regulators: hnRNP-A1 (Kashima et al., 2007a; Kashima et al., 2007b; Doktor et al., 2011; Harahap et al., 2012), SF2/ASF (SRSF1) (Cartegni and Krainer, 2002; Cartegni et al., 2006; Wee et al., 2014), hTra2β1 (SRSF10) (Helmken and Wirth, 2000; Hofmann et al., 2000; Hofmann and Wirth, 2002; Chen et al., 2015), SaM68 (KHDRBS1) (Pedrotti et al., 2010; Pagliarini et al., 2015), and SRp20 (SRSF3) (Helmken et al., 2003). The transcript levels of these splicing factors were measured in type II SMA fibroblasts treated with NHE inhibitors or DMSO for 5 days. *hnRNP-A1* transcript levels were significantly reduced in GM03813 cells treated with DMA, EIPA, HMA, and zoniporide (Fig. 6A). DMA, EIPA, HMA, and cariporide reduced *SF2/ASF* levels in SMA fibroblasts (Fig. 6B). Cariporide was the only NHE inhibitor to increase *hTra2β1* mRNA levels (Fig. 6C). HMA significantly reduced *SaM68* transcript levels in SMA fibroblasts (Fig. 6D). EIPA, HMA, cariporide, and zoniporide decreased *SRp20* mRNA levels, whereas DMA increased *SRp20* transcript levels (Fig. 6E). Interestingly, *hrRNP-A1*, *hTra2β1*, and *SRp20* mRNA levels are significantly elevated in GM03813 type II SMA fibroblasts relative to GM03814 carrier fibroblasts (Fig. 6, A, C, and E). Although the NHE inhibitors differentially regulate the expression of splicing factors that regulate *SMN2* exon 7 inclusion, there was no correlation between the differential expression of any of these splicing factors and the enhanced inclusion of *SMN2* exon 7 induced by EIPA or HMA in SMA fibroblasts.

Identification of Differentially Expressed Transcripts in SMA Fibroblasts Treated with EIPA. To understand the molecular mechanisms by which EIPA enhances *SMN2* exon 7 inclusion, we compared the transcriptomes of GM03813 type II SMA fibroblasts treated with 10 μM EIPA against those treated with DMSO as well as against those treated with 10 μM amiloride, which did not increase *SMN2* exon 7 inclusion. Principal component analysis correctly distributed each of the samples within their treatment groups (Fig. 7A). Hierarchical clustering of the identified transcripts from amiloride-treated (Fig. 7B) and EIPA-treated (Fig. 7C) fibroblasts showed consistent differential expression between each treatment group. Amiloride treatment of GM03813 SMA fibroblasts altered the levels of 1269 transcripts when compared against DMSO-treated cells (Fig. 7D; Supplemental Table 1A). There were 999 differentially expressed transcripts in SMA fibroblasts treated with 10 μM EIPA when compared against those cells exposed to DMSO (Fig. 7E; Supplemental Table 1B). To identify those differentially expressed transcripts that may be relevant to *SMN2* alternative splicing, we compared the EIPA transcriptome against the amiloride transcriptome and identified 839 EIPA-unique differentially expressed transcripts (Fig. 7F; Supplemental Table 1C).

Ingenuity Pathways Analysis (Krämer et al., 2014) uses a manually curated literature database to determine the biologic relevance of differentially expressed transcripts. There were 165 canonical pathways that were significantly overrepresented (Fisher's exact test P value ≤ 0.05) in EIPA-treated SMA fibroblasts relative to amiloride-treated cells (Supplemental Table 2), with the top 12 overrepresented pathways shown in Fig. 7G. Most of the top 12 overrepresented pathways contained Ras-family GTPases (*RAP2A*, *RAP1A*, and *MRAS*) and subunits of the phosphatidylinositol-4-phosphate 3-kinase (*PIK3R1*, *PIK3C2G*, and *PIK3CB*). Upstream regulator analysis (Krämer et al., 2014) can identify potential upstream molecules that may be responsible for EIPA-mediated differential gene expression. UPA identified 19 potential upregulators (10 of which were activated and 9 were inhibited) in EIPA-treated SMA fibroblasts relative to amiloride-treated fibroblasts (Fig. 7H; Supplemental Table 3). Thrombospondin-1 (*THBS1*) and *DHCR7* are overrepresented target molecules in this analysis.

Transcriptome arrays can also provide important information about differential splicing in response to drug treatment. There were 10,307 splicing events that were differentially expressed in amiloride-treated GM03813 SMA fibroblasts, whereas EIPA treatment showed 8307 differentially expressed splicing events. Of those events, only 352 were classifiable as either intron retention, alternative 5′ donor, alternative 3′ acceptor, or cassette exon events in amiloride-treated cells and

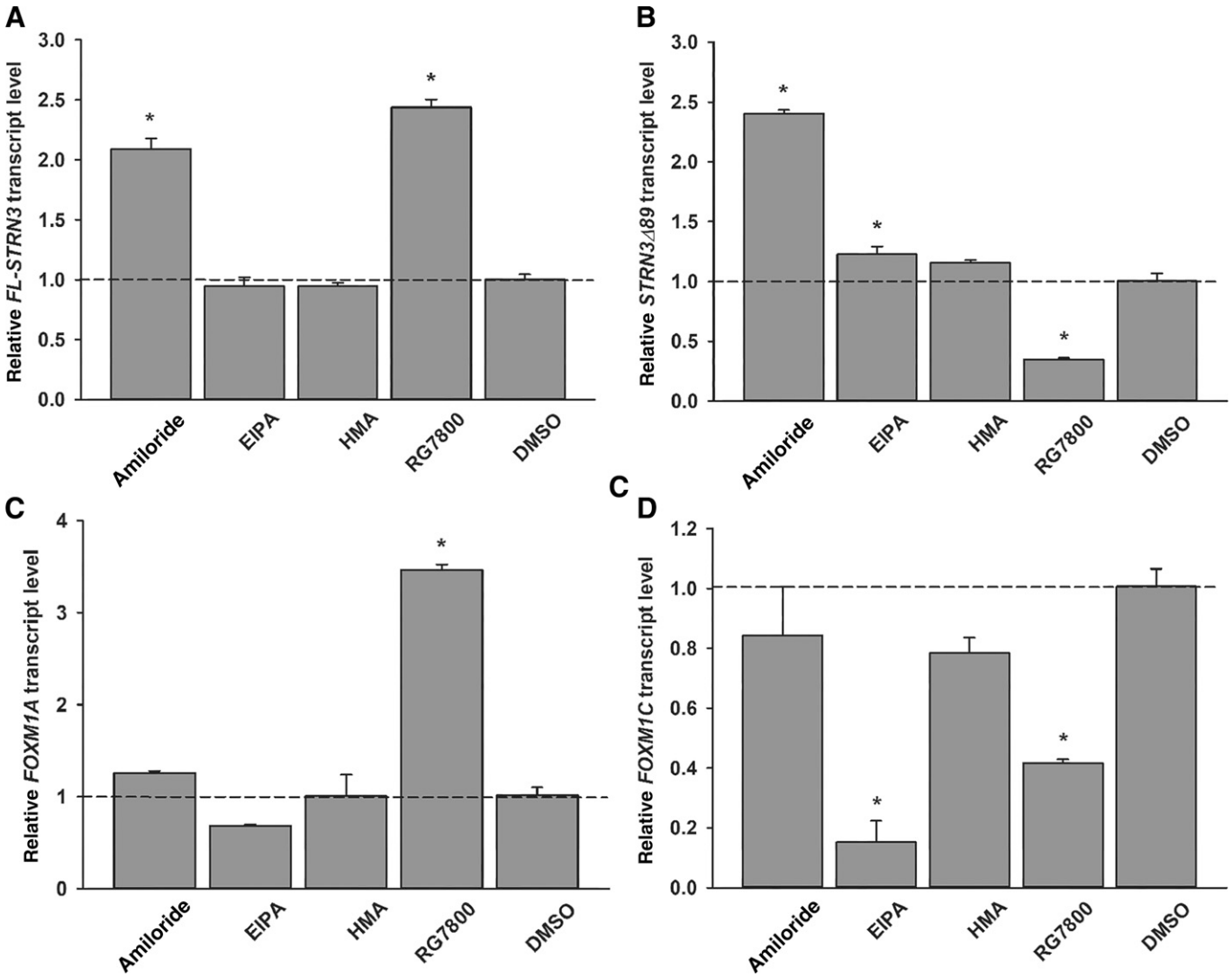

Fig. 5. Effects of the NHE inhibitors on alternative splicing of STRN3 and FOXM1 in type II SMA fibroblasts. GM03813 type II SMA fibroblasts were treated with 10 μM amiloride, 10 μM EIPA, 10 μM HMA, 1 μM RG7800, or DMSO (n = 3 per group) for 5 days. The levels of *FL-STRN3* (A), *STRN3Δ89* (B), *FOXM1* containing exons Va and VIIa [*FOXM1A* (C)], and *FOXM1* containing exon Va [*FOXM1C*; (D)] transcripts were measured in total RNA extracted from treated cells by quantitative RT-PCR. All transcript levels were expressed relative to DMSO-treated GM03813 cells (dashed line). The asterisk (*) denotes a statistically significant ($P < 0.05$) difference between drug- and vehicle-treated cells.

251 in EIPA-treated cells (Fig. 7I). The splicing index (SI) is a measure of exon expression that is normalized to the expression level of that gene (Clark et al., 2007). In EIPA-treated cells, there was an increase in the *SMN2* exons 6 and 7 splice junction (JUC0500051219; SI = +2.34, P = 0.0031) and a decrease in *SMN2* exons 6 and 8 splice junction (JUC0500051223; SI = -2.68; P = 0.0086). Amiloride treatment, however, did not significantly alter the abundance of either splice junction. The amount of *SMN2* exon 7 inclusion was, therefore, increased in EIPA-treated SMA fibroblasts.

To validate our microarray analysis, we used biologic replicates of type II SMA fibroblasts (Fang and Cui, 2011) that were treated with either 10 μM EIPA, 10 μM HMA, 10 μM amiloride, 1 μM RG7800, or DMSO. We focused on the following transcripts: *TIA1* (Fig. 8A; 2.06-fold decrease), *FABP3* (Fig. 8B; 6.44-fold increase), *DHCR7* (Fig. 8C; 2.07-fold decrease), *TRPV4* (Fig. 8D; 2.13-fold decrease), *ATXN1* (Fig. 8E; 2.58-fold decrease), and *PRKAR2B* (Fig. 8F; 2.15-fold increase). The differential expressions of these transcripts, with respect to direction, in response to EIPA treatment were validated in the biologic replicates. Transcripts that are differentially expressed only in EIPA- and HMA-treated SMA fibroblasts would potentially provide insights into the molecular mechanisms underlying EIPA- and HMA-induced *SMN2* exon 7 inclusion. *FABP3* (Fig. 8B) transcript levels were markedly increased in cells treated with EIPA and HMA but not with amiloride or RG7800. EIPA and HMA as well as RG7800 reduced *TIA1* transcript levels (Fig. 8A) in SMA fibroblasts. For the remaining transcripts, the direction of change in response to EIPA treatment was different from that to HMA, i.e., increased in EIPA-treated cells but decreased in HMA-treated cells.

Discussion

Because of the inverse relationship between SMA severity and *SMN2* copy number, *SMN2* is a primary target of SMA treatment and drug discovery through multiple

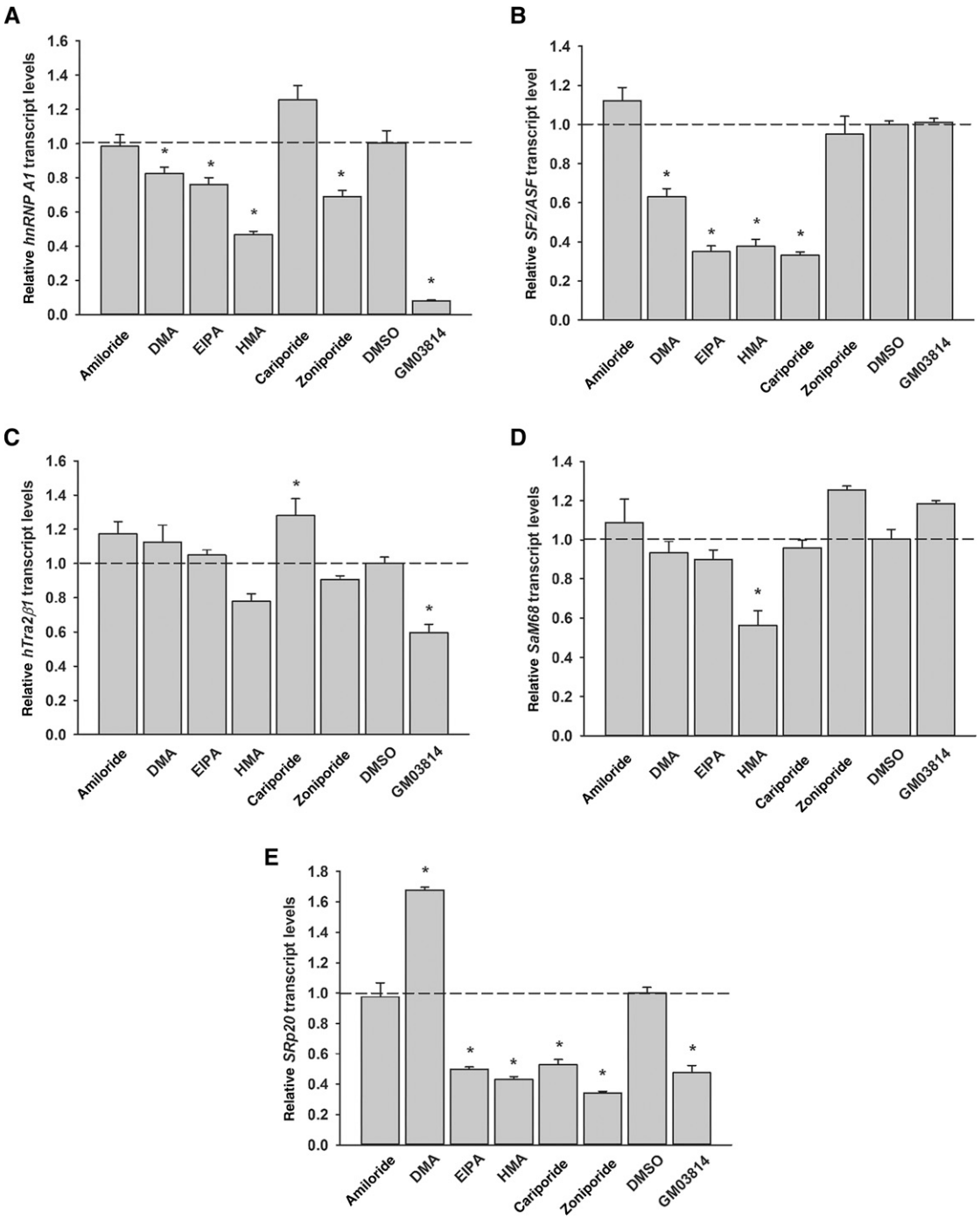

Fig. 6. Effects of NHE inhibitors on the expression of splicing regulators involved in SMN2 exon 7 alternative splicing. GM03813 type II SMA fibroblasts were treated with 10 μM NHE inhibitors (amiloride, DMA, EIPA, HMA, cariporide, or zoniporide) or DMSO (n = 3 per group) for 5 days. *hnRNP*-A1 (A), SF2/ASF (B), hTRA2β1 (C), SaM68 (D), and SRp20 (E) transcript levels were measured in total RNA extracted from treated cells by quantitative RT-PCR. Transcript levels were also measured in GM03814 carrier fibroblasts. All transcript levels were expressed relative to DMSO-treated GM03813 cells (dashed line). The asterisk (*) denotes a statistically significant ($P < 0.05$) difference between drug- and vehicle-treated cells.

mechanisms including promoter activation and increased exon 7 inclusion of *SMN2* pre-mRNA transcripts (Cherry et al., 2014). Many structurally distinct small molecules such as EIPA (Yuo et al., 2008), the pyridopyrimidinones RG7800 and RG7916 (Naryshkin et al., 2014; Feng et al., 2016; Ratni et al., 2016; Woll et al., 2016; Sivaramakrishnan et al., 2017; Ratni et al., 2018; Wang et al., 2018), and NVS-SM1 (Palacino et al., 2015) increase *SMN2* expression by enhancing exon 7 inclusion. EIPA is a derivative of amiloride and inhibits the activity of the SLC9A family of Na^+/H^+ antiporters (Kleyman and Cragoe, 1988). In this study, we examined the effects of amiloride derivatives like EIPA and HMA as well as other NHE inhibitors on *SMN2* alternative splicing of exon 7. EIPA and HMA but none of the other SCL9A inhibitors tested increase *SMN2* exon 7 inclusion via a novel mechanism not involving previously identified regulators of SMN2 exon 7 splicing.

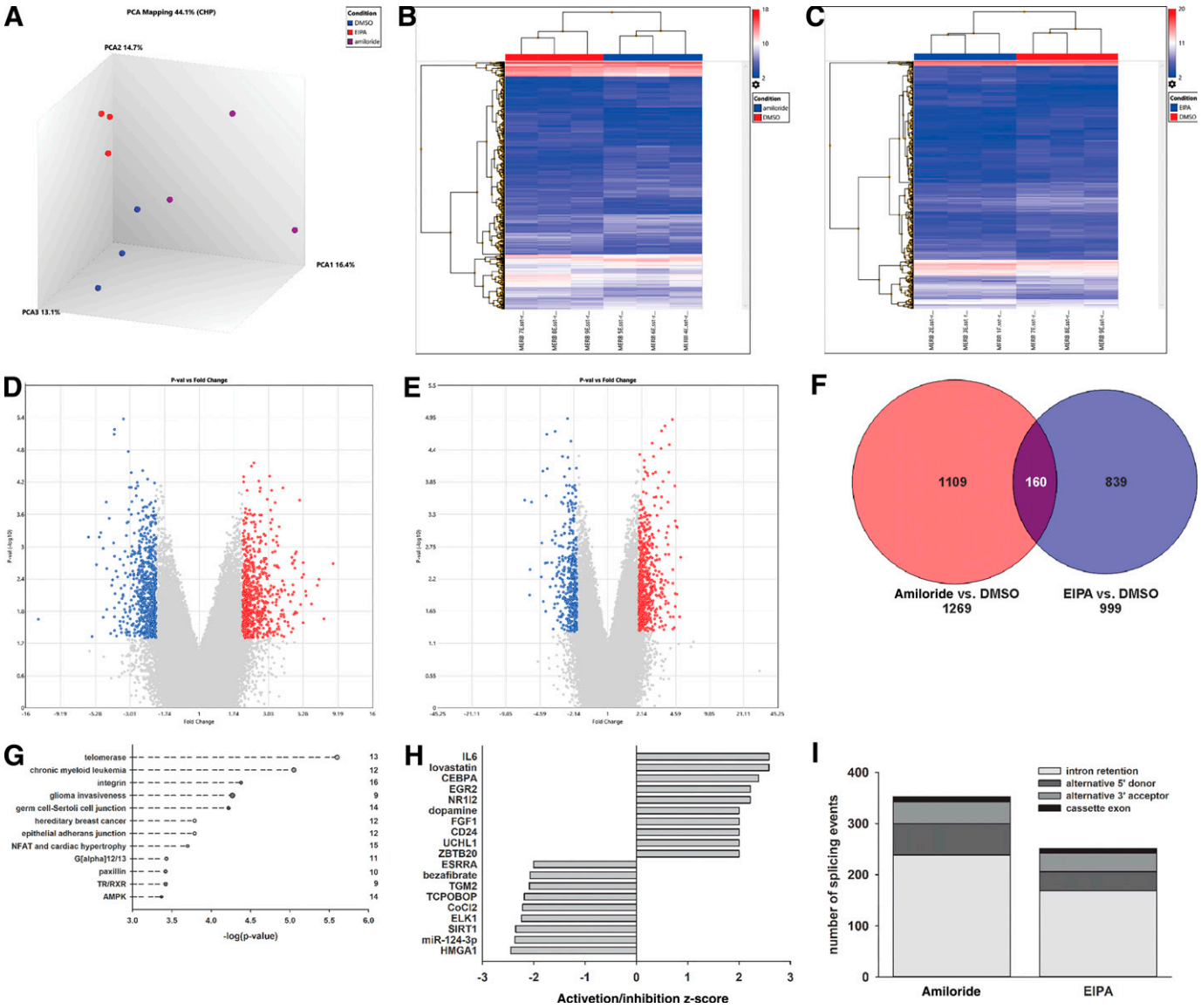

Fig. 7. Identification of differentially expressed transcripts in type II SMA fibroblasts treated with amiloride or EIPA. GM03813 type II SMA fibroblasts were treated with 10 μM amiloride, 10 μM EIPA, or DMSO (n = 3 per group) for 5 days, and their RNA pools were analyzed for differential transcript expression using Clariom D human transcriptome arrays. (A) Principal component analysis of samples treated with amiloride (purple), EIPA (red), or DMSO (blue). Hierarchical clustering analysis of amiloride versus DMSO (B) and EIPA versus DMSO (C). Volcano plots of amiloride versus DMSO (D) and EIPA versus DMSO (E) type II SMA fibroblast transcriptomes. Significantly upregulated transcripts are shown in red, and significantly downregulated transcripts are shown in blue. (F) Venn diagram showing the similarities and differences between the amiloride versus DMSO (red) and EIPA versus DMSO (blue) transcriptomes. The overlap between these two transcriptomes is shown in purple. (G) The top dozen canonical pathways—out of 165—that were significantly over-represented in the EIPA-unique transcriptome. The numbers next to the pathway lines represent the number of differentially expressed molecules for each pathway. (H) The upstream regulators that are significantly and uniquely differentially regulated in EIPA-treated type II SMA fibroblasts. (I) Distributions of the categorized differential splicing events between amiloride versus DMSO and EIPA versus DMSO transcriptomes.

There are 5 different isoforms of SLC9A-type Na^+/H^+ antiporters that are localized to the plasma membrane in mammalian cells (Masereel et al., 2003). NHE1 is ubiquitously expressed in most mammalian cell types, whereas NHE5 is primarily expressed in neurons and skeletal muscle (Donowitz et al., 2013). Tissue distribution profiles of *NHE1* and *NHE5* in humans and mice show strong expression in the tissues from which the cell lines used in this study were derived, i.e., brain and skin (Fagerberg et al., 2014; Yue et al., 2014; Cheng et al., 2019). EIPA and the related amiloride analog HMA are potent inhibitors of the NHE1 and NHE5 isoforms (Kleyman and Cragoe, 1988; Szabó et al., 2000; Masereel et al., 2003). Cariporide and zoniporide, on the other hand, are selective inhibitors of NHE1 (Masereel et al., 2003).

EIPA modulates neuronal plasticity and long-term potentiation in mice (Rönicke et al., 2009). NHE5 has been shown to be involved in neuronal excitation and long-term potentiation by negatively regulating dendrite spine growth in an activity-dependent manner (Diering et al., 2011). NHE5 knockout mice display enhanced learning and memory and increased BDNF/TrkB-mediated signaling (Chen et al., 2017). NHE5 also regulates the membrane trafficking of the receptor tyrosine kinase Met and β1 integrins in glioma cells (Fan et al., 2016; Kurata et al., 2019). NHE5 is positively regulated by

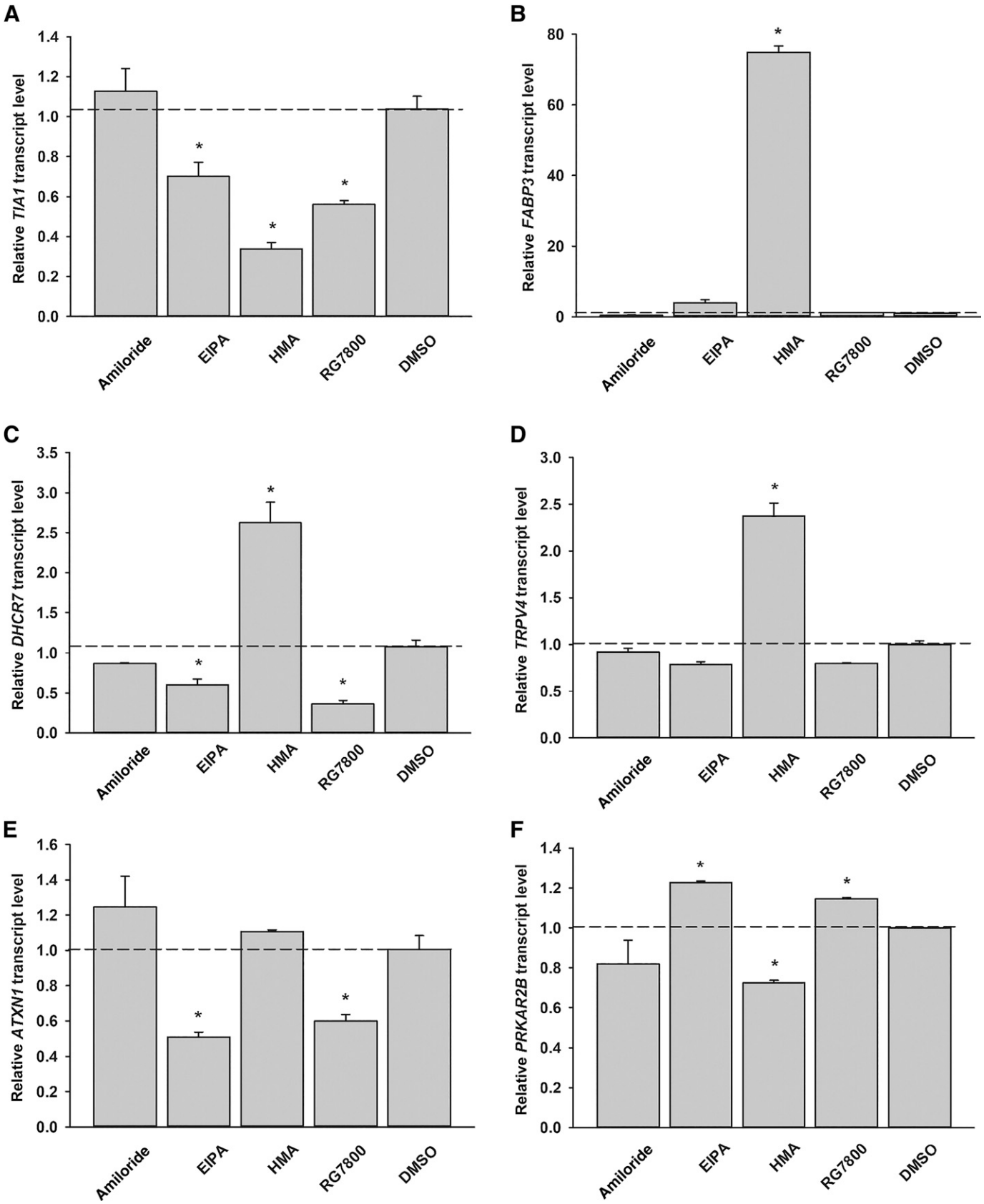

Fig. 8. Validation of EIPA- and HMA-responsive transcripts in type II SMA fibroblasts. GM03813 type II SMA fibroblasts were treated with 10 μM amiloride, 10 μM EIPA, 10 μM HMA, 1 μM RG7800, or DMSO (n = 3 per group) for 5 days. *TIA1* (A), *FABP3* (B), *DHCR7* (C), *TRPV4* (D), *ATXN1* (E), and *PRKARB2* (F) transcript levels were measured in total RNA extracted from treated cells by quantitative RT-PCR. All transcript levels were expressed relative to DMSO-treated GM03813 cells (dashed line). The asterisk (*) denotes a statistically significant ($P < 0.05$) difference between drug- and vehicle-treated cells.

AMP-activated protein kinase (AMPK) in neuronal as well as nonneuronal cells (Jinadasa et al., 2014). NHE5 membrane localization is regulated by phosphatidylinositol 3-kinase (PI3K) activity and the actin cytoskeleton (Szászi et al., 2002). In addition to these roles in neuronal signaling, NHE5 regulates autophagy in neuronal cells (Togashi et al., 2013). Based on our observations, the selectivity of EIPA and HMA in increasing *SMN2* exon 7 inclusion may result from inhibition of a specific NHE isoform, in this case *NHE5*. The regulation of alternative splicing by *NHE5* has not been previously reported; future studies using gene knockdown approaches in SMA model systems will further elucidate the role of *NHE5* in *SMN2* exon 7 splicing. It is possible that selective inhibition of *NHE5* may not be sufficient to increase *SMN2* exon 7 inclusion. To address this possibility, future studies would determine if inhibition of other NHE isoforms, like *NHE1*, would be necessary for or would augment *SMN2* alternative splicing resulting from inhibition of *NHE5*.

The pyridopyridinone RG7800—which is undergoing clinical trials with SMA patients—increases *SMN2* exon 7 inclusion by binding to an exonic splice enhancer (ESE2) element present on the 5′ splice site of the exon 7:intron 7 junction (Ratni et al., 2016; Woll et al., 2016; Sivaramakrishnan et al., 2017). Binding at these sites facilitates the binding of U1 small nuclear ribonucleoproteins by dissociation of the inhibitory splicing factor hnRNP-G. *STRN3* has a similar pre-mRNA structure to the *SMN2* exon 7:intron 7 junction, and RG7800 increases the inclusion of *STRN3* exons 8 and 9 (Naryshkin et al., 2014; Sivaramakrishnan et al., 2017). We show that EIPA and HMA have no effect on exon 8 and 9 inclusion in *STRN3* transcripts. Furthermore, EIPA and HMA do not modulate the alternative splicing of *FOXM1*, another transcript whose splicing is modulated by RG7800 (Ratni et al., 2018). These data suggest that EIPA and HMA modulate *SMN2* exon 7 alternative splicing via a mechanism that is distinct from the pyridopyridinones.

NHE antiporters regulate the cellular pH in mammalian cells (Putney et al., 2002; Masereel et al., 2003). Alterations in pH have been shown to affect the splicing of multiple mRNA transcripts including tenascin C and *SMN2* (Borsi et al., 1995; Chen et al., 2008). Low extracellular pH increases *SMN2* exon 7 skipping, whereas a high extracellular pH promotes exon 7 inclusion (Chen et al., 2008). The decrease in exon 7 inclusion at low pH may be the result of diminished nuclear localization of hnRNP-A1, a splicing factor that prevents exon 7 inclusion via binding to an exonic enhancer element (Chen et al., 2008). EIPA (Yuo et al., 2008) and elevating extracellular pH (Chen et al., 2008) increase the nuclear localization of the splicing factor SRp20. In this study, we did not identify any relationship between the differential expression of any of these splicing factors and the enhanced inclusion of *SMN2* exon 7 induced by EIPA or HMA in SMA fibroblasts. Furthermore, the effects of EIPA and HMA on *SMN2* exon 7 alternative splicing may not be linked with regulation of cellular pH as other NHE1-selective inhibitors like cariporide and zoniporide do not alter *SMN2* exon 7 splicing. The effects of EIPA and HMA on *SMN2* alternative splicing may be mediated by a novel mechanism.

TIA1 is a splicing factor that has been shown to increase *SMN2* exon 7 levels (Singh et al., 2011). Loss of *Tia1* worsens disease progression in female, but not male, SMA-like mice (Howell et al., 2017). We show here that EIPA and HMA decrease *TIA1* mRNA levels in SMA fibroblasts even though these compounds increase *SMN2* exon 7 inclusion. Muscle biopsies from patients with Welander distal myopathy that harbor a point mutation in *TIA1* [TIA1(E384K)] have reduced *FL-SMN2* transcript levels but elevated *SMNΔ7* transcript levels (Klar et al., 2013); however, a recent report (Carrascoso et al., 2018) has shown that mutant TIA1 only modestly affects *SMN2* exon 7 alternative splicing in different cell types. Future studies will elucidate the role of NHE5 inhibition by EIPA and HMA on *TIA1* expression and the regulation of *TIA1* expression on the modulation *SMN2* exon 7 alternative splicing.

FABP3 transcript levels were markedly elevated in SMA fibroblasts treated with EIPA or HMA but not by other NHE inhibitors. *FABP3* is robustly expressed in neurons, as well as other nonneural tissues, and is responsible for intracellular transport of long-chain polyunsaturated fatty acids (Liu et al., 2010; Falomir-Lockhart et al., 2019). FABP3 increases the aggregation of α-synuclein within dopaminergic neurons of the substantia nigra pars compacta, which leads to cell death and neurodegeneration (Shioda et al., 2014). In murine GABAergic neurons within the anterior cingulate cortex, FABP3 modulates the expression of glutamic acid decarboxylase (*Gad67*) by differential promoter methylation (Yamamoto et al., 2018). Further studies examining the effect of increased *FABP3* expression on *SMN2* alternative splicing would provide important insights into a novel mechanism of gene regulation.

Although EIPA and HMA are potent inhibitors of NHE-type antiporters (Masereel et al., 2003), it is possible their mode of action with respect to *SMN2* exon 7 inclusion may be separate from NHE inhibition. Certain amilorides can also inhibit different types of Ca^{2+}-activated nonspecific cation channels like acid-sensing ion channel 1A or transient receptor potential P3, also known as polycystin-2 (Dai et al., 2007; Leng et al., 2016). It is possible that the effects of EIPA and HMA on *SMN2* alternative splicing may be mediated by inhibition of these other channels. To address this possibility, SMA fibroblasts and other cellular models can be treated with more specific acid-sensing ion channel 1A or transient receptor potential P3 inhibitors, like phenamil and benzamil (Dai et al., 2007; Leng et al., 2016), to monitor their effects on *SMN2* exon 7 inclusion.

SMA can now be considered an actionable disease since there are currently 3 therapies approved by the FDA for SMA patients: nusinersen (Finkel et al., 2017; Mercuri et al., 2018), risdiplam (Baranello et al., 2021), and onasemnogene abeparvovec (Mendell et al., 2017). Despite these exciting advances, other therapies are needed, particularly if they are complementary to current therapeutic options. Traditional small-molecule therapies have been the mainstay of the pharmaceutical industry for several important reasons. Small molecule inducers of *SMN2* expression could serve as complementary therapies for SMA patients who are either not good candidates or poor responders to biologic therapies. NHE5 inhibitors like EIPA and HMA may be able to serve this complementary role, but they will need to be tested in animal models for SMA. The identification of more precise targets for therapeutic development will ultimately lead to additional drug candidates for the treatment of SMA, which can be used either alone or in combination with existing SMA therapies.

Acknowledgments

The authors would like to thank Dr. Norman Gerry and the staff at Advanced BioMedical Laboratories, LLC (Cinnaminson, NJ) for completing the microarray experiments; Vertex Pharmaceuticals, Inc. for generously providing the NSC34:SMN2.Mg2.bla5.3 reporter cell line; and the Nemours Biomolecular Core Laboratory for access to the 7900HT Fast Real-Time PCR system.

Note Added in Proof: The title of this article was changed from that used in the Fast Forward version that appeared online June 6, 2022.

Authorship Contributions

Participated in research design: Kanda, Butchbach.

Conducted experiments: Kanda, Moulton.

Contributed new reagents or analytic tools: Butchbach.

Performed data analysis: Kanda, Moulton, Butchbach.

Wrote or contributed to the writing of the manuscript: Kanda, Moulton, Butchbach.

References

Andreassi C, Jarecki J, Zhou J, Coovert DD, Monani UR, Chen X, Whitney M, Pollok B, Zhang M, Androphy E, et al. (2001) Aclarubicin treatment restores SMN levels to cells derived from type I spinal muscular atrophy patients. *Hum Mol Genet* **10**:2841–2849.

Baranello G, Darras BT, Day JW, Deconinck N, Klein A, Masson R, Mercuri E, Rose K, El-Khairi M, Gerber M, et al.; FIREFISH Working Group (2021) Risdiplam in type 1 spinal muscular atrophy. *N Engl J Med* **384**:915–923.

Barrett T, Wilhite SE, Ledoux P, Evangelista C, Kim IF, Tomashevsky M, Marshall KA, Phillippy KH, Sherman PM, Holko M, et al. (2013) NCBI GEO: archive for functional genomics data sets–update. *Nucleic Acids Res* **41**:D991–D995.

Borsi L, Balza E, Gaggero B, Allemanni G, and Zardi L (1995) The alternative splicing pattern of the tenascin-C pre-mRNA is controlled by the extracellular pH. *J Biol Chem* **270**:6243–6245.

Burnett BG, Muñoz E, Tandon A, Kwon DY, Sumner CJ, and Fischbeck KH (2009) Regulation of SMN protein stability. *Mol Cell Biol* **29**:1107–1115.

Butchbach MER (2016) Copy number variations in the *Survival Motor Neuron* genes: implications for spinal muscular atrophy and other neurodegenerative diseases. *Front Mol Biosci* **3**:7.

Calder AN, Androphy EJ, and Hodgetts KJ (2016) Small molecules in development for the treatment of spinal muscular atrophy. *J Med Chem* **59**:10067–10083.

Carrascoso I, Sánchez-Jiménez C, Silion E, Alcalde J, and Izquierdo JM (2018) A heterologous cell model for studying the role of T-cell intracellular antigen 1 in Welander distal myopathy. *Mol Cell Biol* **39**:e00299–218.

Cartegni L, Hastings ML, Calarco JA, de Stanchina E, and Krainer AR (2006) Determinants of exon 7 splicing in the spinal muscular atrophy genes, *SMN1* and *SMN2*. *Am J Hum Genet* **78**:63–77.

Cartegni L and Krainer AR (2002) Disruption of an SF2/ASF-dependent exonic splicing enhancer in *SMN2* causes spinal muscular atrophy in the absence of *SMN1*. *Nat Genet* **30**:377–384.

Chen X, Wang X, Tang L, Wang J, Shen C, Liu J, Lu S, Zhang H, Kuang Y, Fei J, et al. (2017) Nhe5 deficiency enhances learning and memory via upregulating Bdnf/TrkB signaling in mice. *Am J Med Genet B Neuropsychiatr Genet* **174**:828–838.

Chen YC, Chang JG, Jong YJ, Liu TY, and Yuo CY (2015) High expression level of Tra2-β1 is responsible for increased *SMN2* exon 7 inclusion in the testis of SMA mice. *PLoS One* **10**:e0120721.

Chen YC, Yuo CY, Yang WK, Jong YJ, Lin HH, Chang YS, and Chang JG (2008) Extracellular pH change modulates the exon 7 splicing in *SMN2* mRNA. *Mol Cell Neurosci* **39**:268–272.

Cheng PC, Lin HY, Chen YS, Cheng RC, Su HC, and Huang RC (2019) The Na^+/H^+-exchanger NHE1 regulates extra- and intracellular pH and nimodipine-sensitive $[Ca^{2+}]_i$ in the suprachiasmatic nucleus. *Sci Rep* **9**:6430.

Cherry JJ, Kobayashi DT, Lynes MM, Naryshkin NN, Tiziano FD, Zaworski PG, Rubin LL, and Jarecki J (2014) Assays for the identification and prioritization of drug candidates for spinal muscular atrophy. *Assay Drug Dev Technol* **12**:315–341.

Cho S and Dreyfuss G (2010) A degron created by *SMN2* exon 7 skipping is a principal contributor to spinal muscular atrophy severity. *Genes Dev* **24**:438–442.

Clark TA, Schweitzer AC, Chen TX, Staples MK, Lu G, Wang H, Williams A, and Blume JE (2007) Discovery of tissue-specific exons using comprehensive human exon microarrays. *Genome Biol* **8**:R64.

Crawford TO and Pardo CA (1996) The neurobiology of childhood spinal muscular atrophy. *Neurobiol Dis* **3**:97–110.

Cuscó I, Barceló MJ, Soler C, Parra J, Baiget M, and Tizzano E (2002) Prenatal diagnosis for risk of spinal muscular atrophy. *BJOG* **109**:1244–1249.

Dai XQ, Ramji A, Liu Y, Li Q, Karpinski E, and Chen XZ (2007) Inhibition of TRPP3 channel by amiloride and analogs. *Mol Pharmacol* **72**:1576–1585.

Diering GH, Mills F, Bamji SX, and Numata M (2011) Regulation of dendritic spine growth through activity-dependent recruitment of the brain-enriched Na^+/H^+ exchanger NHE5. *Mol Biol Cell* **22**:2246–2257.

Doktor TK, Schroeder LD, Vested A, Palmfeldt J, Andersen HS, Gregersen N, and Andresen BS (2011) *SMN2* exon 7 splicing is inhibited by binding of hnRNP A1 to a common ESS motif that spans the 3′ splice site. *Hum Mutat* **32**:220–230.

Donowitz M, Ming Tse C, and Fuster D (2013) SLC9/NHE gene family, a plasma membrane and organellar family of Na^+/H^+ exchangers. *Mol Aspects Med* **34**:236–251.

Fagerberg L, Hallström BM, Oksvold P, Kampf C, Djureinovic D, Odeberg J, Habuka M, Tahmasebpoor S, Danielsson A, Edlund K, et al. (2014) Analysis of the human tissue-specific expression by genome-wide integration of transcriptomics and antibody-based proteomics. *Mol Cell Proteomics* **13**:397–406.

Falomir-Lockhart LJ, Cavazzutti GF, Giménez E, and Toscani AM (2019) Fatty acid signaling mechanisms in neural cells: fatty acid receptors. *Front Cell Neurosci* **13**:162.

Fan SHY, Numata Y, and Numata M (2016) Endosomal Na^+/H^+ exchanger NHE5 influences MET recycling and cell migration. *Mol Biol Cell* **27**:702–715.

Fang Z and Cui X (2011) Design and validation issues in RNA-seq experiments. *Brief Bioinform* **12**:280–287.

Feng Z, Ling KKY, Zhao X, Zhou C, Karp G, Welch EM, Naryshkin N, Ratni H, Chen KS, Metzger F, et al. (2016) Pharmacologically induced mouse model of adult spinal muscular atrophy to evaluate effectiveness of therapeutics after disease onset. *Hum Mol Genet* **25**:964–975.

Finkel RS, Mercuri E, Darras BT, Connolly AM, Kuntz NL, Kirschner J, Chiriboga CA, Saito K, Servais L, Tizzano E, et al.; ENDEAR Study Group (2017) Nusinersen versus sham control in infantile-onset spinal muscular atrophy. *N Engl J Med* **377**:1723–1732.

Gentillon C, Connell AJ, Kirk RW, and Butchbach MER (2017) The effects of C5-substituted 2,4-diaminoquinazolines on selected transcript expression in spinal muscular atrophy cells. *PLoS One* **12**:e0180657.

Harahap ISK, Saito T, San LP, Sasaki N, Gunadi, Nurputra DKP, Yusoff S, Yamamoto T, Morikawa S, Nishimura N, et al. (2012) Valproic acid increases *SMN2* expression and modulates SF2/ASF and hnRNPA1 expression in SMA fibroblast cell lines. *Brain Dev* **34**:213–222.

Heier CR, Gogliotti RG, and DiDonato CJ (2007) SMN transcript stability: could modulation of messenger RNA degradation provide a novel therapy for spinal muscular atrophy? *J Child Neurol* **22**:1013–1018.

Helmken C, Hofmann Y, Schoenen F, Oprea G, Raschke H, Rudnik-Schöneborn S, Zerres K, and Wirth B (2003) Evidence for a modifying pathway in SMA discordant families: reduced SMN level decreases the amount of its interacting partners and Htra2-beta1. *Hum Genet* **114**:11–21.

Helmken C and Wirth B (2000) Exclusion of Htra2-β1, an up-regulator of full-length SMN2 transcript, as a modifying gene for spinal muscular atrophy. *Hum Genet* **107**:554–558.

Hofmann Y, Lorson CL, Stamm S, Androphy EJ, and Wirth B (2000) Htra2-β 1 stimulates an exonic splicing enhancer and can restore full-length *SMN* expression to *survival motor neuron 2* (*SMN2*). *Proc Natl Acad Sci USA* **97**:9618–9623.

Hofmann Y and Wirth B (2002) hnRNP-G promotes exon 7 inclusion of *survival motor neuron* (SMN) via direct interaction with Htra2-β1. *Hum Mol Genet* **11**:2037–2049.

Howell MD, Ottesen EW, Singh NN, Anderson RL, Seo J, Sivanesan S, Whitley EM, and Singh RN (2017) TIA1 is a gender-specific disease modifier of a mild mouse model of spinal muscular atrophy. *Sci Rep* **7**:7183.

Hsieh-Li HM, Chang JG, Jong YJ, Wu MH, Wang NM, Tsai CH, and Li H (2000) A mouse model for spinal muscular atrophy. *Nat Genet* **24**:66–70.

Jinadasa T, Szabó EZ, Numat M, and Orlowski J (2014) Activation of AMP-activated protein kinase regulates hippocampal neuronal pH by recruiting $Na(^+)/H(^+)$ exchanger NHE5 to the cell surface. *J Biol Chem* **289**:20879–20897.

Kashima T, Rao N, David CJ, and Manley JL (2007a) hnRNP A1 functions with specificity in repression of *SMN2* exon 7 splicing. *Hum Mol Genet* **16**:3149–3159.

Kashima T, Rao N, and Manley JL (2007b) An intronic element contributes to splicing repression in spinal muscular atrophy. *Proc Natl Acad Sci USA* **104**:3426–3431.

Klar J, Sobol M, Melberg A, Mäbert K, Ameur A, Johansson ACV, Feuk L, Entesarian M, Orlén H, Casar-Borota O, et al. (2013) Welander distal myopathy caused by an ancient founder mutation in *TIA1* associated with perturbed splicing. *Hum Mutat* **34**:572–577.

Kleyman TR and Cragoe Jr EJ (1988) Amiloride and its analogs as tools in the study of ion transport. *J Membr Biol* **105**:1–21.

Krämer A, Green J, Pollard Jr J, and Tugendreich S (2014) Causal analysis approaches in Ingenuity Pathway Analysis. *Bioinformatics* **30**:523–530.

Kurata T, Rajendran V, Fan S, Ohta T, Numata M, and Fushida S (2019) NHE5 regulates growth factor signaling, integrin trafficking, and degradation in glioma cells. *Clin Exp Metastasis* **36**:527–538.

Lefebvre S, Bürglen L, Reboullet S, Clermont O, Burlet P, Viollet L, Benichou B, Cruaud C, Millasseau P, Zeviani M, et al. (1995) Identification and characterization of a spinal muscular atrophy-determining gene. *Cell* **80**:155–165.

Leng TD, Si HF, Li J, Yang T, Zhu M, Wang B, Simon RP, and Xiong ZG (2016) Amiloride analogs as ASIC1a inhibitors. *CNS Neurosci Ther* **22**:468–476.

Liao GB, Li XZ, Zeng S, Liu C, Yang SM, Yang L, Hu CJ, and Bai JY (2018) Regulation of the master regulator FOXM1 in cancer. *Cell Commun Signal* **16**:57.

Liu RZ, Mita R, Beaulieu M, Gao Z, and Godbout R (2010) Fatty acid binding proteins in brain development and disease. *Int J Dev Biol* **54**:1229–1239.

Lorson CL and Androphy EJ (2000) An exonic enhancer is required for inclusion of an essential exon in the SMA-determining gene SMN. *Hum Mol Genet* **9**:259–265.

Lorson CL, Hahnen E, Androphy EJ, and Wirth B (1999) A single nucleotide in the *SMN* gene regulates splicing and is responsible for spinal muscular atrophy. *Proc Natl Acad Sci USA* **96**:6307–6311.

Maeda M, Harris AW, Kingham BF, Lumpkin CJ, Opdenaker LM, McCahan SM, Wang W, and Butchbach MER (2014) Transcriptome profiling of spinal muscular atrophy motor neurons derived from mouse embryonic stem cells. *PLoS One* **9**:e106818.

Masereel B, Pochet L, and Laeckmann D (2003) An overview of inhibitors of $Na(^+)/H(^+)$ exchanger. *Eur J Med Chem* **38**:547–554.

Mendell JR, Al-Zaidy S, Shell R, Arnold WD, Rodino-Klapac LR, Prior TW, Lowes L, Alfano L, Berry K, Church K, et al. (2017) Single-dose gene-replacement therapy for spinal muscular atrophy. *N Engl J Med* **377**:1713–1722.

Mercuri E, Darras BT, Chiriboga CA, Day JW, Campbell C, Connolly AM, Iannaccone ST, Kirschner J, Kuntz NL, Saito K, et al.; CHERISH Study Group (2018)

Nusinersen versus sham control in later-onset spinal muscular atrophy. *N Engl J Med* **378**:625–635.

Michaud M, Arnoux T, Bielli S, Durand E, Rotrou Y, Jablonka S, Robert F, Giraudon-Paoli M, Riessland M, Mattei MG, et al. (2010) Neuromuscular defects and breathing disorders in a new mouse model of spinal muscular atrophy. *Neurobiol Dis* **38**:125–135.

Monani UR, Lorson CL, Parsons DW, Prior TW, Androphy EJ, Burghes AHM, and McPherson JD (1999) A single nucleotide difference that alters splicing patterns distinguishes the SMA gene *SMN1* from the copy gene *SMN2*. *Hum Mol Genet* **8**:1177–1183.

Monani UR, Sendtner M, Coovert DD, Parsons DW, Andreassi C, Le TT, Jablonka S, Schrank B, Rossoll W, Prior TW, et al. (2000) The human centromeric survival motor neuron gene (*SMN2*) rescues embryonic lethality in *Smn(-/-)* mice and results in a mouse with spinal muscular atrophy [published correction appears in *Hum Mol Genet* (2007) 16:2648]. *Hum Mol Genet* **9**:333–339.

Naryshkin NA, Weetall M, Dakka A, Narasimhan J, Zhao X, Feng Z, Ling KKY, Karp GM, Qi H, Woll MG, et al. (2014) Motor neuron disease. SMN2 splicing modifiers improve motor function and longevity in mice with spinal muscular atrophy. *Science* **345**:688–693.

Pagliarini V, Pelosi L, Bustamante MB, Nobili A, Berardinelli MG, D'Amelio M, Musarò A, and Sette C (2015) SAM68 is a physiological regulator of *SMN2* splicing in spinal muscular atrophy. *J Cell Biol* **211**:77–90.

Palacino J, Swalley SE, Song C, Cheung AK, Shu L, Zhang X, Van Hoosear M, Shin Y, Chin DN, Keller CG, et al. (2015) *SMN2* splice modulators enhance U1-pre-mRNA association and rescue SMA mice. *Nat Chem Biol* **11**:511–517.

Pearn J (1978) Incidence, prevalence, and gene frequency studies of chronic childhood spinal muscular atrophy. *J Med Genet* **15**:409–413.

Pedrotti S, Bielli P, Paronetto MP, Ciccosanti F, Fimia GM, Stamm S, Manley JL, and Sette C (2010) The splicing regulator Sam68 binds to a novel exonic splicing silencer and functions in *SMN2* alternative splicing in spinal muscular atrophy. *EMBO J* **29**:1235–1247.

Pfaffl MW (2001) A new mathematical model for relative quantification in real-time RT-PCR. *Nucleic Acids Res* **29**:e45.

Putney LK, Denker SP, and Barber DL (2002) The changing face of the Na^+/H^+ exchanger, NHE1: structure, regulation, and cellular actions. *Annu Rev Pharmacol Toxicol* **42**:527–552.

Ratni H, Ebeling M, Baird J, Bendels S, Bylund J, Chen KS, Denk N, Feng Z, Green L, Guerard M, et al. (2018) Discovery of Risdiplam, a Selective Survival of Motor Neuron-2 (SMN2) Gene Splicing Modifier for the Treatment of Spinal Muscular Atrophy (SMA). *J Med Chem* **61**:6501–6517.

Ratni H, Karp GM, Weetall M, Naryshkin NA, Paushkin SV, Chen KS, McCarthy KD, Qi H, Turpoff A, Woll MG, et al. (2016) Specific Correction of Alternative Survival Motor Neuron 2 Splicing by Small Molecules: Discovery of a Potential Novel Medicine To Treat Spinal Muscular Atrophy. *J Med Chem* **59**:6086–6100.

Rönicke R, Schröder UH, Böhm K, and Reymann KG (2009) The Na^+/H^+ exchanger modulates long-term potentiation in rat hippocampal slices. *Naunyn Schmiedebergs Arch Pharmacol* **379**:233–239.

Schmittgen TD and Livak KJ (2008) Analyzing real-time PCR data by the comparative $C_{(T)}$ method. *Nat Protoc* **3**:1101–1108.

Scudiero DA, Polinsky RJ, Brumback RA, Tarone RE, Nee LE, and Robbins JH (1986) Alzheimer disease fibroblasts are hypersensitive to the lethal effects of a DNA-damaging chemical. *Mutat Res* **159**:125–131.

Shioda N, Yabuki Y, Kobayashi Y, Onozato M, Owada Y, and Fukunaga K (2014) FABP3 protein promotes α-synuclein oligomerization associated with 1-methyl-1,2,3,6-tetrahydropiridine-induced neurotoxicity. *J Biol Chem* **289**: 18957–18965.

Singh NN, Seo J, Ottesen EW, Shishimorova M, Bhattacharya D, and Singh RN (2011) TIA1 prevents skipping of a critical exon associated with spinal muscular atrophy. *Mol Cell Biol* **31**:935–954.

Sivaramakrishnan M, McCarthy KD, Campagne S, Huber S, Meier S, Augustin A, Heckel T, Meistermann H, Hug MN, Birrer P, et al. (2017) Binding to SMN2 pre-mRNA-protein complex elicits specificity for small molecule splicing modifiers. *Nat Commun* **8**:1476.

Stabley DL, Harris AW, Holbrook J, Chubbs NJ, Lozo KW, Crawford TO, Swoboda KJ, Funanage VL, Wang W, Mackenzie W, et al. (2015) *SMN1* and *SMN2* copy numbers in cell lines derived from patients with spinal muscular atrophy as measured by array digital PCR. *Mol Genet Genomic Med* **3**:248–257.

Stabley DL, Holbrook J, Harris AW, Swoboda KJ, Crawford TO, Sol-Church K, and Butchbach MER (2017) Establishing a reference dataset for the authentication of spinal muscular atrophy cell lines using STR profiling and digital PCR. *Neuromuscul Disord* **27**:439–446.

Sumner CJ and Crawford TO (2018) Two breakthrough gene-targeted treatments for spinal muscular atrophy: challenges remain. *J Clin Invest* **128**: 3219–3227.

Szabó EZ, Numata M, Shull GE, and Orlowski J (2000) Kinetic and pharmacological properties of human brain $Na(^+)/H(^+)$ exchanger isoform 5 stably expressed in Chinese hamster ovary cells. *J Biol Chem* **275**:6302–6307.

Szászi K, Paulsen A, Szabó EZ, Numata M, Grinstein S, and Orlowski J (2002) Clathrin-mediated endocytosis and recycling of the neuron-specific Na^+/H^+ exchanger NHE5 isoform. Regulation by phosphatidylinositol 3′-kinase and the actin cytoskeleton. *J Biol Chem* **277**:42623–42632.

Tisdale S and Pellizzoni L (2015) Disease mechanisms and therapeutic approaches in spinal muscular atrophy. *J Neurosci* **35**:8691–8700.

Togashi K, Wakatsuki S, Furuno A, Tokunaga S, Nagai Y, and Araki T (2013) Na^+/H^+ exchangers induce autophagy in neurons and inhibit polyglutamine-induced aggregate formation. *PLoS One* **8**:e81313.

Wang J, Schultz PG, and Johnson KA (2018) Mechanistic studies of a small-molecule modulator of SMN2 splicing. *Proc Natl Acad Sci USA* **115**:E4604–E4612.

Wee CD, Havens MA, Jodelka FM, and Hastings ML (2014) Targeting SR proteins improves SMN expression in spinal muscular atrophy cells. *PLoS One* **9**:e115205.

Woll MG, Qi H, Turpoff A, Zhang N, Zhang X, Chen G, Li C, Huang S, Yang T, Moon YC et al. (2016) Discovery and optimization of small molecule splicing modifiers of survival motor neuron 2 as a treatment for spinal muscular atrophy. *J Med Chem* **59**:6070–6085.

Yamamoto Y, Kida H, Kagawa Y, Yasumoto Y, Miyazaki H, Islam A, Ogata M, Yanagawa Y, Mitsushima D, Fukunaga K, et al. (2018) FABP3 in the anterior cingulate cortex modulates the methylation status of the glutamic acid $decarboxylase_{67}$ promoter region. *J Neurosci* **38**:10411–10423.

Yuan JS, Wang D, and Stewart Jr CN (2008) Statistical methods for efficiency adjusted real-time PCR quantification. *Biotechnol J* **3**:112–123.

Yue F, Cheng Y, Breschi A, Vierstra J, Wu W, Ryba T, Sandstrom R, Ma Z, Davis C, Pope BD, et al.; Mouse ENCODE Consortium (2014) A comparative encyclopedia of DNA elements in the mouse genome. *Nature* **515**:355–364.

Yuo CY, Lin HH, Chang YS, Yang WK, and Chang JG (2008) 5-(N-ethyl-N-isopropyl)-amiloride enhances SMN2 exon 7 inclusion and protein expression in spinal muscular atrophy cells. *Ann Neurol* **63**:26–34.

Address correspondence to: Dr. Matthew E.R. Butchbach, Division of Neurology, Nemours Children's Hospital Delaware, 4462 E400 DuPont Experimental Station, 200 Powder Mill Road, Wilmington, DE 19803. E-mail: matthew.butchbach@nemours.org